



Universiteit
Leiden
The Netherlands

No Haploinsufficiency but Loss of Heterozygosity for EXT in Multiple Osteochondromas

Reijnders, C.M.A.; Waaijer, C.J.F.; Hamilton, A.; Buddingh, E.P.; Dijkstra, S.P.D.; Ham, J.; ... ; Bovee, J.V.M.G.

Citation

Reijnders, C. M. A., Waaijer, C. J. F., Hamilton, A., Buddingh, E. P., Dijkstra, S. P. D., Ham, J., ... Bovee, J. V. M. G. (2010). No Haploinsufficiency but Loss of Heterozygosity for EXT in Multiple Osteochondromas. *American Journal Of Pathology*, 177(4), 1946-1957.
doi:10.2353/ajpath.2010.100296

Version: Not Applicable (or Unknown)
License: [Leiden University Non-exclusive license](#)
Downloaded from: <https://hdl.handle.net/1887/109763>

Note: To cite this publication please use the final published version (if applicable).

Molecular Pathogenesis of Genetic and Inherited Diseases

No Haploinsufficiency but Loss of Heterozygosity for *EXT* in Multiple Osteochondromas

Christianne M.A. Reijnders,*
Cathelijin J.F. Waaijer,* Andrew Hamilton,[†]
Emilie P. Buddingh,[‡] Sander P.D. Dijkstra,[§]
John Ham,[¶] Egbert Bakker,^{||} Karoly Szuhai,**
Marcel Karperien,^{††} Pancras C.W. Hogendoorn,*
Sally E. Stringer,[†] and Judith V.M.G. Bovée*

From the Departments of Pathology,* Pediatrics,[‡] Orthopedic Surgery,[§] Human and Clinical Genetics,^{||} and Molecular Cell Biology,** Leiden University Medical Center, Leiden, The Netherlands; the Section of Cardiovascular Medicine, School of Biomedicine, Faculty of Medical and Human Sciences,[†] Manchester Academic Health Science Centre (CMFT), University of Manchester, Manchester, United Kingdom; the Department of Orthopedics,[¶] Onze Lieve Vrouwe Gasthuis (OLVG), Amsterdam, The Netherlands; and the MIRA Institute for Biomedical Technology and Technical Medicine,^{††} Department of Tissue Regeneration, University of Twente, Enschede, The Netherlands

Multiple osteochondromas (MO) is an autosomal dominant disorder caused by germline mutations in *EXT1* and/or *EXT2*. In contrast, solitary osteochondroma (SO) is nonhereditary. Products of the *EXT* gene are involved in heparan sulfate (HS) biosynthesis. In this study, we investigated whether osteochondromas arise via either loss of heterozygosity (2 hits) or haploinsufficiency. An *in vitro* three-dimensional chondrogenic pellet model was used to compare heterozygous bone marrow-derived mesenchymal stem cells (MSCs *EXT*^{wt/-}) of MO patients with normal MSCs and the corresponding tumor specimens (presumed *EXT*^{-/-}). We demonstrated a second hit in *EXT* in five of eight osteochondromas. HS chain length and structure, *in vitro* chondrogenesis, and *EXT* expression levels were identical in both *EXT*^{wt/-} and normal MSCs. Immunohistochemistry for HS, HS proteoglycans, and HS-dependent signaling pathways (eg, TGF- β /BMP, Wnt, and PTHLH) also showed no differences. The cartilaginous cap of osteochondroma contained a mixture of HS-positive and HS-negative cells. Because a heterozygous *EXT* mutation does not affect chondrogenesis, *EXT*, HS, or downstream signaling pathways in MSCs, our results refute the haploinsufficiency theory. We found a second hit in 63% of analyzed osteochondromas, support-

ing the hypothesis that osteochondromas arise via loss of heterozygosity. The detection of the second hit may depend on the ratio of HS-positive (normal) versus HS-negative (mutated) cells in the cartilaginous cap of the osteochondroma. (Am J Pathol 2010, 177:1946–1957; DOI: 10.2353/ajpath.2010.100296)

Osteochondromas (OCs) are benign cartilage forming tumors, which are present at the surface of the long bones.¹ OCs manifest and increase in size the first decade of life. The growth of OCs ceases during puberty when the growth plate closes. Multiple osteochondromas (MO), previously known as hereditary multiple exostoses, is an autosomal dominant disorder, caused by mutations in the tumor suppressor genes *EXT1* or *EXT2*.^{2,3} The main complication is transformation toward malignancy, which occurs in 0.5 to 5% of the patients.^{2–4}

According to Knudson's two-hit model for tumor suppressor genes,⁵ both alleles should be inactivated for OC formation in MO and solitary osteochondroma (SO) patients. Loss of heterozygosity of *EXT1* and/or *EXT2* was shown in solitary OCs,^{6–8} in hereditary OCs,⁷ and in secondary peripheral CS,^{7,9–11} supporting the two-hit model. However, in a considerable proportion of the MO patients loss of the remaining wild-type allele has not been detected,^{12–14} resulting in a longstanding discussion in the literature as to whether OCs in MO patients could arise through haploinsufficiency.

The *EXT* gene products catalyze heparan sulfate (HS) biosynthesis in the Golgi apparatus by elongation of the HS chains.^{15–18} *EXT* and HS proteoglycans (HSPGs) are essential for the diffusion of the morphogens Hedgehog

Supported by Netherlands Organization for Scientific Research (917-76-315 to C.M.A.R. and J.V.M.G.B.) and British Heart Foundation (FS/05/060 to S.E.S.). This study was performed within the context of the EuroBoNet consortium (018814), a European Commission granted Network of Excellence for studying the pathology and genetics of bone tumors.

Accepted for publication June 7, 2010.

Supplemental material for this article can be found on <http://ajp.amjpathol.org>.

Address reprint requests to Judith V. M. G. Bovée, M.D., Ph.D., Department of Pathology, Leiden University Medical Center, PO Box 9600, L1-Q, 2300 RC Leiden, The Netherlands. E-mail: j.v.m.g.bovee@lumc.nl.

(Hh), decapentaplegic (dpp, human homologues transforming growth factor [TGF]- β and bone morphogenic protein [BMP]) and wingless (wg, human homologue wnt).^{19–22} These downstream pathways of EXT play an important role in development and in endochondral bone formation. During normal growth, Indian hedgehog (Ihh) and parathyroid hormone-like hormone (PTHrP) regulate proliferation and differentiation of chondrocytes of the growth plate. In OCs the function of the *EXT* genes is impaired. This might lead to accumulation of HSPGs in the Golgi apparatus and cytoplasm of the OC chondrocytes,²³ which is followed by disturbed downstream pathways of EXT. We and others previously showed that the Ihh pathway is active in OCs,^{24,25} while the PTHrP signaling, regulating chondrocyte proliferation, is absent in OCs and up-regulated on malignant transformation.^{26,27} Wnt signaling and TGF- β signaling are also active in the majority of the OCs.²⁵

In this study our aim was to investigate whether OCs arise via the classical two-hit model for tumor suppressor genes or via haploinsufficiency (gene dosage model, ie, the loss of one *EXT* allele). So, we first determined whether the second hit was present in the cartilage cap of MO and SO patients. Subsequently, we used an *in vitro* 3D chondrogenic pellet model in which bone marrow-derived mesenchymal stem cells (MSCs) of healthy donors and SO patients (*EXT*^{wt/wt}) were compared with MSCs of MO patients (*EXT*^{wt/-}) and tissue from the cartilage cap of MO and SO patients (presumed *EXT*^{-/-}). MSCs 3D *in vitro* pellets provide a suitable model to study chondrogenesis. We investigated *EXT* expression, HS structure and chain length, and RNA and protein expression of members of the EXT downstream pathways in the different EXT conditions.

Materials and Methods

Patient Material

Different specimens of resected OC cartilage cap of MO patients ($n = 8$) and SO patients ($n = 3$) were collected: ie, fresh frozen material, formalin-fixed paraffin-embedded material (after decalcification by either EDTA or formic acid), and tissue processed for cell culturing. From the same patients as well as from healthy donors ($n = 3$) MSCs were isolated from bone marrow (0.5–5 ml). Samples were obtained during surgery at two different hospitals (Leiden University Medical Center [LUMC] and Onze Lieve Vrouwe Gasthuis [OLVG]). Additionally, blood samples of MO patients were collected to isolate lymphocyte DNA, and *EXT1* and *EXT2* mutation analysis was performed as described.^{28,29} Patient characteristics are summarized in Table 1. All specimens were obtained after informed consent and approval of the Ethical Medical Committee (P07.078) of the LUMC and OLVG. Post-natal growth plate samples had previously been collected from resections or biopsies for orthopedic clinical conditions not related to osteochondroma or chondrosarcoma.²³ All samples were handled according to the eth-

ical guidelines as described in the Code for Proper Secondary Use of Human Tissue in The Netherlands of the Dutch Federation of Medical Scientific Societies.

EXT Mutation Analysis and DNA Tiling Array

Normal lymphocyte DNA of MO patients and DNA isolated from the dissected cartilaginous caps of the OCs were sequenced and compared.²⁸ The SO specimens were hybridized on a custom made oligonucleotide array.³⁰ Tumor percentage was >70% except for L2467 (<50%). The number of genes spotted on the array has been extended to 144 genes selected for their function in cartilage biosynthesis (Supplemental Table 1, available at <http://ajp.amjpathol.org>). Sequence data and DNA tiling array data were analyzed with Mutation Surveyor (Soft Genetics, LCC, version 3.24, State College, PA) and Nexus (BioDiscovery Inc., version 3.6, El Segundo, CA), respectively.

Cell Culture

Monolayer Culture

MSCs were expanded in low-glucose (1 g/L) DMEM (Invitrogen, Breda, NL) supplemented with 10% fetal bovine serum (HyClone, Thermo Scientific, Etten-Leur, NL) and 2% P/S. Cartilage cap cells were isolated from SO and MO patients and expanded in RPMI (Invitrogen) supplemented with 10% fetal bovine serum (Invitrogen) and 2% P/S (Invitrogen). Cells were kept at 37°C and 5% CO₂. Medium was changed twice a week.

Flow Cytometric Analysis MSCs

Flow cytometric analysis was performed for all MSC samples at passage 3 to 6 to confirm that adherent cells expanded from the bone marrow were MSCs. Monoclonal antibodies used were anti-CD86-FITC (1:40), anti-HLA-DR FITC (1:30), anti-CD31-PE (1:200), anti-CD34-PE (1:120), anti-CD73-PE (1:25), anti-CD90-PE (1:500), anti-CD3-PerCPCY5.5 (1:10), and anti-CD45-PerCPCY5.5 (1:200; all Becton Dickinson, Franklin Lakes, NJ), and anti-CD105-PE (1:40; Ancell, Bayport, MN). Cells were harvested using trypsin/EDTA (Invitrogen) and washed with 0.5% BSA/PBS and incubated with the respective antibodies for 20 minutes at 4°C. Flow cytometry was performed using a FACS Calibur System (Becton Dickinson) and results were analyzed using CellQuest Pro Software (Becton Dickinson).

Adipogenic and Osteogenic Differentiation

To establish the multipotent differentiation capacity of the MSCs (adipogenic and osteogenic) a subset of MSCs ($n = 4$) was tested in duplicate. Cells were seeded at a density of 15,000 cells per cm² in 0.1% gelatin coated plates and cultured in α -MEM (Lonza, Breda, NL) with 10% FCS, 1% Glutamax (Invitrogen), 1% P/S, dexamethasone (10^{-7}

Table 1. Patient Characteristics with *EXT* Mutations and *EXT* Levels

ID	M, F	Age	N, SO, MO	OC, PCSI	Location	Germline	Tumor	<i>EXT1</i> *	<i>EXT2</i> *	HS (10E4) [†]
L2069	M	11	MO	OC	Tibia; femur	<i>EXT1</i> , exon 1 c.538_539delAG, p.Ser180fsX7	Heterozygous	0.36	1.17	Nd
L2227	F	13	MO	OC	Tibia; femur	<i>EXT1</i> , exon 1 c.364C>T, p.Gln122X and c.373G>T, p.Glu125X	Homozygous	0.17	0.91	~50%
L2232	M	39	MO	OC	Femur	<i>EXT1</i> , exon 8 c.1696G>T, p.Glu566X	Nd	Nd	Nd	~60%
L2254	M	43	MO	PCSI	Os pubis	<i>EXT2</i> , exon 6 c.980delG, p.Gly327AlafsX5	Homozygous	0.42	BDL	~20%
L2467	F	8	MO	OC	Femur	<i>EXT1</i> , exon 1 c.643_662del, p.Met215GlnfsX	Heterozygous	0.27	1.70	~50%
L2240	M	45	MO	OC	Hip	Mutation analysis: negative; DNA tiling array: 80.7kb deletion intron <i>EXT1</i> , 68.9 kb amplification upstream	Nd	Nd	Nd	Negative
L2352	F	10	MO	OC	Femur	<i>EXT1</i> , del exon 4–11; <i>EXT2</i> , UV ex10 c.1641C>T, p.Asp547Asp	Homozygous	0.43	1.54	~40%
L2378	F	17	MO	OC	Humerus	Mutation analysis: negative; DNA tiling array: none in <i>EXT1/2</i>	Nd	0.20	0.26	~25%
L2084	M	18	SO	OC	Tibia	Nd	Homozygous loss <i>EXT1</i> ; partly hemizygous	0.33	0.66	~15%
L2361	M	37	SO	PCSI	Femur	Nd	Hemizygous loss <i>EXT1</i>	0.32	1.12	~10%
L2370	M	9	SO	OC	Tibia	Nd	Homozygous loss <i>EXT1</i> ; partly hemizygous; homozygous deletion 6p (CNV region)	Nd	Nd	~10%
N1	M	15	N			Nd	—	—	—	—
N3	M	50	N			Nd	—	—	—	—
N4	F	27	N			Nd	—	—	—	—

M indicates male; F, female; N, healthy donor; MO, multiple osteochondromas; SO, solitary osteochondroma; OC, osteochondroma; PCSI, peripheral chondrosarcoma grade I; CNV, copy number variation.

*Relative *EXT1* or *EXT2* mRNA expression of OC as a fraction of the average growth plate expression.

[†]Percentage HS chain (10E4)-positive cells present in cartilage cap; BDL, below detection level; Nd, not determined; N1, N3, N4, healthy donors, no tumor material available.

mol/L; Sigma-Aldrich, Zwijndrecht, NL) and ascorbate-2-phosphate (50 µg/ml; Sigma-Aldrich). Adipogenic medium was supplemented with insulin (100 µg/ml; Sigma-Aldrich), indomethacin (0.5 mmol/L; Sigma-Aldrich) and 1-methyl-3-isobutylxanthine (IBMX; 50 µmol/L; Sigma-Aldrich). Osteogenic medium was supplemented with 5 mmol/L β-glycerolphosphate, which was added to the medium after 7 days of culture. Medium was changed twice a week. After 3 weeks of culture, cells were fixed 10 minutes with 4% paraformaldehyde and stained for 10 minutes with oil red O (3 mg/ml) or 5 minutes with Alizarin red (20 mg/ml) to assess adipogenic and osteogenic differentiation, respectively.

Chondrogenic Differentiation

At 90% confluence, the MSCs or cartilage cap cells were washed, harvested, and pellets were made. Chondrogenic medium consisted of high-glucose (4.5 g/L)

DMEM (Invitrogen), proline (40 µg/ml; Sigma-Aldrich), ITS premix (insulin, human transferrin and selenous acid; 50 mg/ml; Becton Dickinson), sodium pyruvate (100 µg/ml; Sigma-Aldrich), Glutamax (1%) and P/S (final concentration: 100U/ml) supplemented with ascorbate-2-phosphate (50 µg/ml), TGF-β3 (10 ng/ml; R&D Systems, Abingdon, UK), dexamethasone (10⁻⁷ mol/L) and BMP-6 (500 ng/ml, R&D Systems). Cells were seeded at a density of 200,000 cells per U-shaped well in a 96-well plate (50 pellets per time series). Subsequently, plates were centrifuged at 1200 rpm for 7 minutes. Medium was changed twice a week. Pellets were harvested at 2, 4, and 6 weeks.

HS Extraction

To recover intracellular and extracellular HS, cells and media were removed from culture flasks at 70–80% confluence by scraping with a sterile cell scraper. Triton-

X100 (1%; Sigma-Aldrich) and protease (1 mg/ml; Sigma-Aldrich) were added to the cell suspensions and incubated for 16 hours at 55°C. HS extraction was as described by Chen and colleagues.³¹ An additional desalting step using a PD-10 chromatography (GE Healthcare, Little Chalfont, UK) was performed at the end of the protocol to remove residual salts from the sample.

HS Chain Length Analysis

For HS chain length determination, cells were incubated in growth media containing 10 μ Ci/ml glucosamine hydrochloride d-[6-³H(N)] (Perkin Elmer, Waltham, MA) for 24 hours, followed by HS extraction as described above. Further preparation of HS for chain length analysis was performed according to Robinson and colleagues.³² HS chain length was determined by size-exclusion chromatography on a Sepharose CL-6B column (GE Healthcare) using a 10 mmol/L Tris-base, 0.2 mol/L NaCl, pH 7.5 buffer at a flow rate of 4 ml/hour. Fractions were collected at 1 minute intervals. Fractions were mixed with 3 ml Optiphase Hisafe 2 scintillation fluid (Perkin-Elmer) and radiolabeled HS content was determined by scintillation counting (Packard Tri-Carb 2500TR liquid scintillation analyzer [Cannerra, Meriden, CT]). The void and total volumes of column were determined by dextran blue and phenol red, respectively. HS chain length was estimated from calibration data described by Wasteson.³³

SAX-HPLC for Analysis of HS Chain Composition

HS digestion for disaccharide analysis was performed according to Chen and colleagues.³¹ Before loading onto HPLC, 5 μ l Milli-Q water was added to the sample. Disaccharide composition was determined by Strong Anion-exchange (SAX) chromatography on a ProPac PA-1 column (Dionex, Sunnyvale, CA) using postcolumn fluorescent detection. Eluents used were as follows: A, Milli-Q water pH 3.5; B, 1 mol/L NaCl pH 3.5; C, 0.5% 2-cyanoacetamide; D, 0.25 mol/L NaOH. Flow rate was 1 ml/min. The gradient program was as follows: 1 minute. eluent A, 1–45 minutes. 0 to 100% eluent B, 45–55 minutes. 100% eluent B, 55–57 minutes. step-wise decrease of eluent B to 0%, followed by a wash in eluent A for 13 minutes. The eluate was mixed with equal proportions of 0.5% 2-cyanoacetamide (HPLC grade, Fluka, Sigma, Dorset, UK) and 0.25M NaOH (HPLC grade, Sigma) that were dispensed at a flow rate of 0.45 ml/min, and reacted at 122°C in a post column reactor (CRX400, Pickering Laboratories, Mountain View, CA). The eluate was then cooled in line in a cooling tower maintained at approximately 10°C and detected by in-line fluorescence at 346 nm excitation; 410 nm emission. An equal mix (0.16nmol total) of the HS disaccharides: Δ UA-GlcNAc, Δ UA-GlcNS, Δ UA-GlcNAc6S, Δ UA-GlcNS6S, Δ UA2S-GlcNS, and Δ UA2S-GlcNS6S (Seikagaku, Tokyo, Japan) was used to calibrate the equipment. Eluted disaccharides were analyzed using ChemStation software (Agilent Technologies, Santa Clara, CA). Results were analyzed

by the SPSS 16.0 for Windows software package (SPSS Inc., Chicago, IL). Differences in relative HS disaccharide expression as measured by SAX-HPLC were analyzed by independent samples student's *t*-tests. *P* values <0.05 were considered significant.

Histology

Pellets were fixed in 4% paraformaldehyde covered by Cytoblock (Shandon Cytoblock, Thermo Scientific, Etten-Leur, NL) and embedded in paraffin. Subsequently, 3- μ m sections were cut, the middle of the pellets was determined, and sections were mounted onto APES-coated slides. Cartilage formation was assessed by hematoxylin and eosin (HE) and toluidine blue staining. Metachromasia was measured with the multispectral imaging system (Nuance FX, Cambridge Research & Instrumentation, Inc [CRI], Woburn, MA) on the microscope (Leica DM4000B). This system enabled us to spectral unmix different wavelengths (range, 420–720 nm) and thereby distinguish the purple and blue staining. Finally, we measured the optical density of the unmixed pictures (ImageJ, U.S. National Institutes of Health, Bethesda, MD,) and calculated the ratio purple/blue.

Glycosaminoglycan (GAG) Analysis

GAGs were isolated from pellets by incubation with 0.1 mmol/L EDTA/PBS and 20 μ g proteinase K (Invitrogen, Breda, NL) at 56°C overnight. GAG amounts were then measured by using the Blyscan Sulfated GAG Assay (Biocolor, Carrickfergus, UK) and normalized against DNA content according to the manufacturer's protocol.

Immunohistochemistry

Used antibodies, antibody concentrations, antigen retrieval, positive controls, and other antibody specifications are described in Table 2.³⁴ Negative controls (PBS instead of first antibody) were included for all immunohistochemical stainings. The sections were evaluated according to staining intensity (1 = weak; 2 = moderate; 3 = strong) and the percentage of positive cells (1 = 0–24%; 2 = 25–49%; 3 = 50–74%; 4 = 75–100%) by two observers independently³⁵ for the center (most differentiated cells) and the periphery (more flattened/spindle cells) of the pellets. Sum score was calculated. One-way analysis of variance with Bonferroni's multiple comparison test was used for statistical analysis. *P* values <0.05 were considered significant.

Quantitative Reverse Transcriptase PCR

Total RNA was isolated from the pellets using TRIzol reagent (Invitrogen) according to the manufacturer's protocol. A polytron homogenizer was used to pulverize the pellets. cDNA was synthesized from 0.5 μ g total RNA per sample as described previously.²⁵ Primers for *EXT1*, *EXT2*, *Ihh* (QT01850177, Qiagen, Venlo, NL),

Table 2. Antibodies Used for Immunohistochemistry

Antigen	Manufacturer	Positive Control	Staining	Antibody Concentration	Antigen Retrieval
Collagen II	NeoMarkers	Growth plate	ECM	1 : 100	Proteinase K + hyaluronidase
Collagen X	Quartett	Growth plate	ECM	1 : 100	Proteinase K + hyaluronidase
SOX9	Atlas	Testis	Nucleus	1 : 100	Citrate
HS chains (10E4)	US Biological	Skin	Membrane; ECM	1 : 400	—
Syndecan2 (10H4)	David, G. ³⁴	Growth plate	Membrane; ECM	1 : 50	—
Syndecan3	Proteintech. Group Inc.	Colorectal carcinoma	Cytoplasm	1 : 200	Citrate; NGS
Syndecan4	Atlas	Placenta	Cytoplasm	1 : 1000	Citrate
Perlecan	Atlas	Placenta	Cytoplasm	1 : 1200	Citrate; NGS
CD44v3	Novocastra	Tonsil	Membrane; cytoplasm	1 : 200	Citrate
Phosphosmad 1,5,8	Cell Signaling	Colon	Nucleus	1 : 100	Citrate; elk milk
Phosphosmad 2	Cell Signaling	Kidney	Nucleus	1 : 125	Citrate; NGS
Beta-catenin	Transduction Biosciences	Skin	Cytoplasm	1 : 2000; 1 : 1600	Citrate
PAI1	American Diagnostics	Cervical carcinoma	Cytoplasm	1 : 200	—
Bcl2	Dako	Tonsil	Cytoplasm	1 : 1000	Citrate
PTHLH	Oncogene	Skin	Cytoplasm	1 : 200	Trypsin 30 minutes
PTHR1	Upstate	Skin	Cytoplasm	1 : 400	Citrate
NDST1	Abcam	Ileum	Cytoplasm	1 : 800	Tris-EDTA

ECM indicates extracellular matrix; NGS, normal goat serum.

PTCH, *SMO*, *GLI1*, *GLI2*, and *GLI3* were described previously.^{23,25} Three house keeping genes, G-coupled protein receptor 108 (*GPR108*), cleavage and polyadenylation specific factor 6 (*CPSF6*) and TATA Box-binding protein (*TBP*), were selected to normalize the expression levels.²⁵

Results

Genetic Analysis of MO Patients and Solitary and Hereditary OCs

Of eight patients clinically documented to have MO, five contained a germline mutation in *EXT1* and one patient demonstrated an *EXT2* mutation in lymphocyte DNA (Table 1). Of the two patients negative at DNA sequencing and MLPA analysis, one demonstrated a germline intronic deletion and gain in the *EXT1* region at DNA tiling array, while the other patient was normal at DNA tiling array. To search for a second hit, we examined DNA derived from the tumor tissue using sequencing analysis, and homozygosity for the mutated allele was found in three of five hereditary cases analyzed (Figure 1, A and B). In solitary OCs, two of three cases showed homozygous deletion of *EXT1* at DNA tiling array (Figure 1, C and D). *EXT1* and *EXT2* mRNA expression was diminished in the majority of the OCs compared to the growth plate mRNA expression (Table 1).

Chondrogenesis of Normal, SO, and MO MSCs

We used the 3D-pellet model of MSCs to study chondrogenesis and to mimic the cartilage cap as closely as possible. This model enables the comparison of signaling in wild-type versus *EXT* heterozygous cells differentiated toward the same cell type. To assess that we indeed cultured MSCs, we performed flow cytometric analysis which confirmed the expression of the MSC markers CD73, CD90, and CD105 and the absence of hematopoietic markers on adherent cells expanded from bone marrow. Moreover, the MSCs had the capacity to undergo adipogenesis and osteogenesis (data not shown). To confirm the neoplastic origin of cells cultured from the cartilaginous cap we assessed the presence of genetic aberrations that were found in the corresponding frozen tissue. Intriguingly, although macroscopically strictly cartilaginous tissue dissected from the cap was used for culturing, the pellets from the cultured cartilage cap cells appeared to be derived from normal cells instead of tumor cells as the 8q alterations that were shown in DNA isolated from frozen tumor tissue using DNA tiling array were absent in the cultured cells (data not shown). These were not used for further analysis. Therefore we used fresh frozen and paraffin embedded tissue from the cartilage cap for comparison with the pellets.

All MSCs were able to undergo chondrogenesis *in vitro*, although there was a large inter-donor variability with regard to pellet size. Deposition of cartilaginous

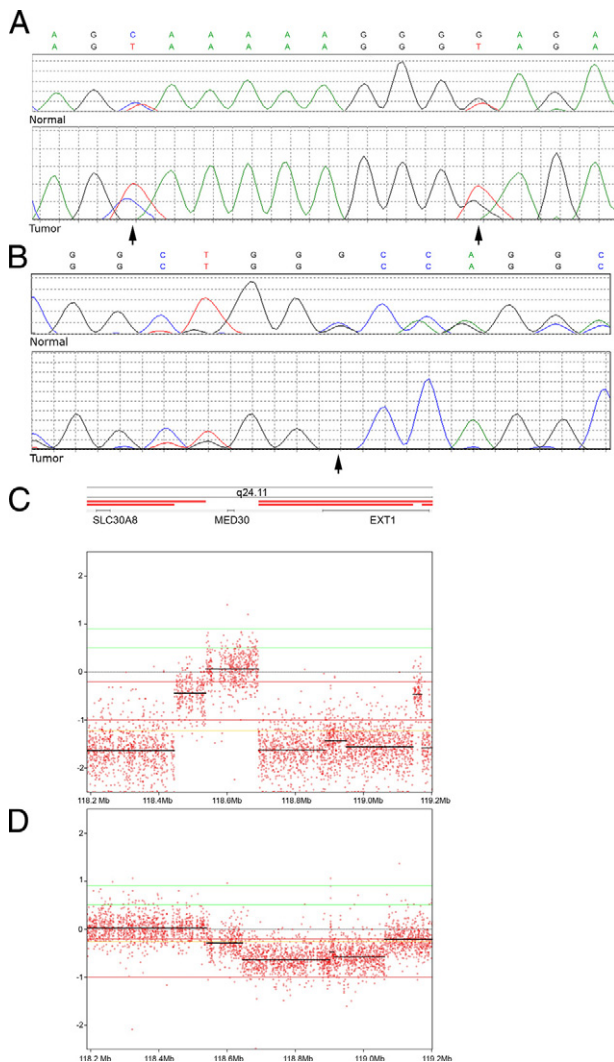


Figure 1. Second hit in hereditary and solitary osteochondromas. **A:** L2227 heterozygous germline mutation in *EXT1*, exon 1 c.364C>T, p.Gln122X, and c.373G>T, p.Glu125X (**upper panel**) with predominance of the sequence of the mutated allele in the tumor DNA (**lower panel, arrows**), suggesting loss of the wild-type allele. **B:** L2254 heterozygous mutation in *EXT2*, exon 6 c.980delG, p.Gly327AlafsX5 in germline (**upper panel**) with homozygosity in the tumor DNA (**lower panel, arrow**). **C** and **D:** DNA tiling results of the solitary tumors, representing the 8q24.11 region and showing a homozygous and partly hemizygous loss of the *EXT1* allele in L2084 (**C**) and L2370 (**D**). Additionally, L2084 also has a homozygous loss of a region near *EXT1*. The values are not as low as expected due to contamination with normal cells.

matrix as determined by metachromasia at toluidine blue staining was shown at 2 weeks in 5/12, at 4 weeks in 11/12, and at 6 weeks in 11/12 pellets (Figure 2, A–C) quantified using the multispectral imaging system (Supplemental Table 2 and Supplemental Figure S1 available at <http://ajp.amjpathol.org>). There were no differences between normal (N), SO (*EXT^{wt/wt}*), and MO (*EXT^{wt/-}*) MSCs. The results were confirmed on protein level using immunohistochemistry for collagen II (Figure 2, D and E). Collagen X expression, indicative of hypertrophic differentiation, was mainly seen at 6 weeks (Figure 2, G and H). Collagen II and X were also expressed in the OCs (Figure 2, F and I). Nuclear SOX9 is highly expressed in all pellets (*EXT^{wt/wt}* and *EXT^{wt/-}*) and OCs (data not shown).

EXT and HS Analysis in *EXT^{wt/wt}* versus *EXT^{wt/-}* MSCs, Pellets, and OCs

We compared the 3D pellets from MSCs of normal donors with those of patients carrying a germline *EXT1* mutation. *EXT1* and *EXT2* mRNA was expressed in all pellets although the levels were variable and lower as compared to growth plate expression (data not shown). Because the *EXT1/EXT2* complex is involved in HS biosynthesis, we analyzed the GAGs. An increase in sulfated GAGs, including HS, was found using the Blyscan method in the *EXT^{wt/wt}* and *EXT^{wt/-}* pellets with increasing culture time. No significant difference of GAG production was found between *EXT^{wt/wt}* and *EXT^{wt/-}* pellets (data not shown). Because *EXT1* and *EXT2* are involved in HS chain length elongation, we determined the HS chain lengths of the *EXT1^{wt/wt}* and *EXT1^{wt/-}* MSCs in monolayer culture (Figure 3, A and B). The HS chains were similar (between 80–120 kDa) and normal in length. HS disaccharide expression also revealed no significant differences between *EXT1^{wt/wt}* and *EXT1^{wt/-}* MSCs (Figure 3, C and D).

Using immunohistochemistry we could additionally compare the *EXT^{wt/wt}* and *EXT^{wt/-}* pellets with tumor tissue, in which *EXT*, at least in solitary OCs,⁸ is presumed to be homozygously inactivated (*EXT^{-/-}*). Immunohistochemistry for HS chains (10E4) demonstrated membranous/cytoplasmic expression of variable intensity in all pellets (Figure 2J). Interestingly, of the cartilaginous caps only 1 of 10 OCs was totally negative for HS expression, whereas 3 of 3 solitary and 6 of 7 hereditary OCs exhibited scattered tumor cells with cytoplasmic and/or nuclear HS chain expression (Table 1; Figure 2, K and L). The percentage of cells positive for 10E4 protein expression was not correlated with age or with detection of loss of heterozygosity, although one should take into account that the analyses were performed on different parts of the tumor; the staining on paraffin tissue and the DNA isolated from frozen tissue. The antibody 10E4 was shown to be specific for HS chains, because after heparitinase treatment (10mU/ml) no HS could be detected (data not shown).

N-deacetylase/n-sulfotransferase 1 (NDST1), an enzyme which is involved in the first step of HS chain modification, was abundantly expressed in the cytoplasm of the *EXT^{wt/wt}* and *EXT^{wt/-}* pellets and the OCs (Table 3). In addition the OCs showed nuclear (Figure 4D) and pericellular ECM NDST1 staining. There was focal NDST1 staining in ECM of the *EXT^{wt/wt}* and *EXT^{wt/-}* pellets (Figure 4A).

HSPG Analysis in *EXT^{wt/wt}* versus *EXT^{wt/-}* Pellets and OCs

Expression of protein cores of HSPGs was studied using immunohistochemistry in pellets and tumor tissue. All HSPGs studied, including syndecans (SDC2–4), perlecan, and CD44v3 (HS bearing variable exon 3 of CD44), were expressed in the cytoplasm of the *EXT^{wt/wt}* and *EXT^{wt/-}* pellets and the OCs (Table 3; Figure 4, B, C, and E–J). The cytoplasmic CD44v3 expression was signifi-

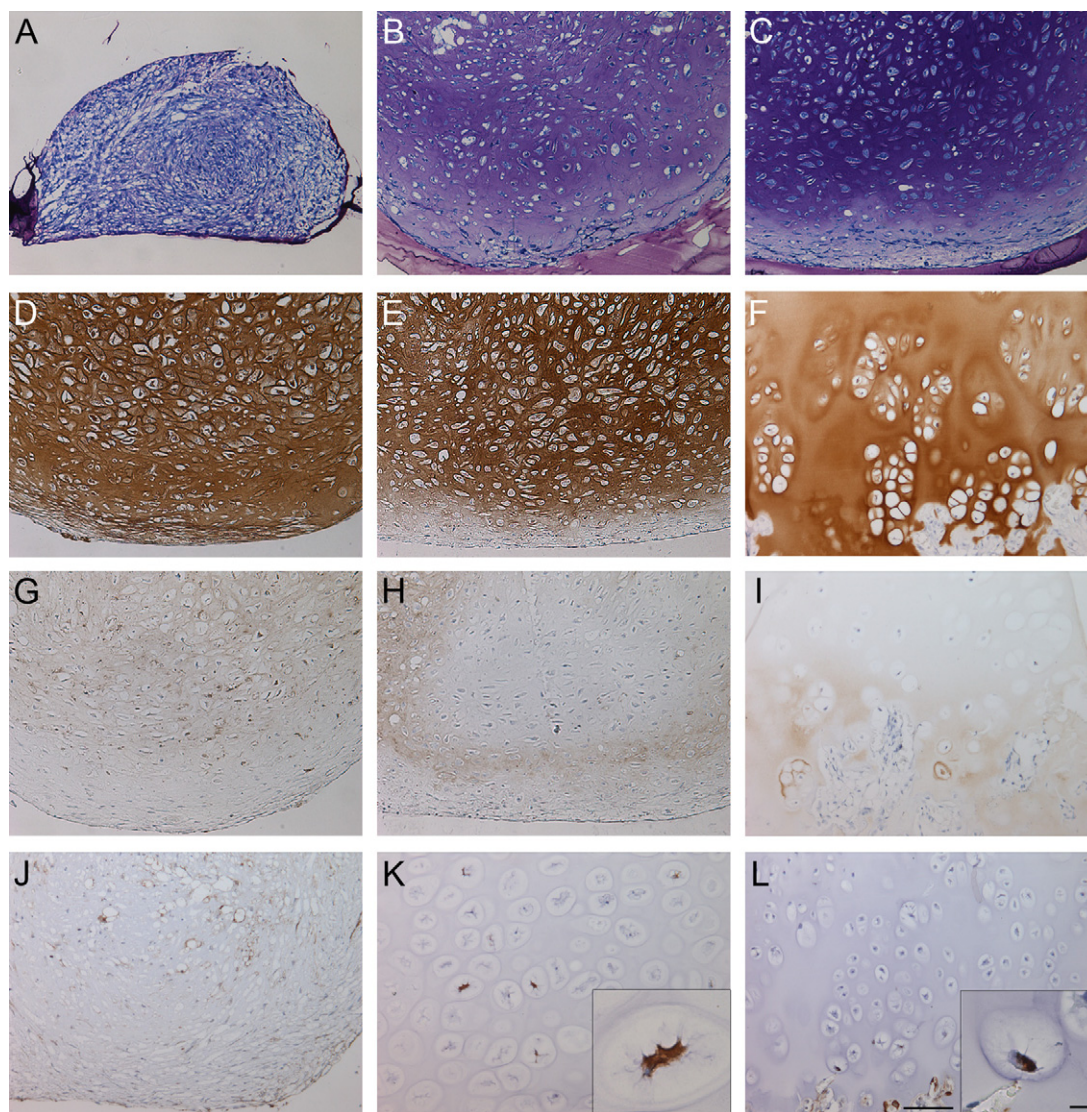


Figure 2. *In vitro* chondrogenesis of normal, SO, and MO MSCs. Toluidine blue staining, *EXT*^{wt/-} pellet after 2, 4, and 6 weeks of culture (**A–C**). Collagen II and collagen X expression, in *EXT*^{wt/wt} pellet, 6 weeks (**D** and **G**); *EXT*^{wt/-} pellet, 6 weeks (**E** and **H**); OC L2370 (**F** and **I**), respectively. Membranous/cytoplasmic HS chain expression in wild-type pellet (**J**). Cytoplasmic HS chain expression in the OCs (**K** and **L**). HS-negative cells are intermingled with either more (L2467, no detection of second hit) (**K**) or fewer 10E4-positive cells (L2370, homozygous loss of *EXT1* detected) (**L**). Scale bars: 100 μ m (**A–L**); 10 μ m (**inset K** and **L**).

cantly ($P < 0.05$) lower in the *EXT*^{wt/wt} and *EXT*^{wt/-} pellets compared to the OCs (Figure 4, G and J). Focal nuclear SDC2, SDC3 and CD44v3 (dot-like) staining was observed in the *EXT*^{wt/wt} and *EXT*^{wt/-} pellets as well as in OCs. The ECM of the *EXT*^{wt/wt} and *EXT*^{wt/-} pellets focally expressed SDC2 and SDC4, whereas the ECM of the OCs had a pericellular ECM expression of SDC3 and perlecan near the ossification zone.

Downstream Signaling Pathways Dependent on HS

IHh Signaling

IHh signaling was active in the pellets and OCs, because the members of the pathway (*IHh*, *PTCH*, *SMO*, *GLI1*, *GLI2*, *GLI3*) were expressed at mRNA level (data not shown). PTHLH signaling, which is downstream of

IHh in normal growth plate, was active in the pellets and OCs because PTHLH and the PTH-receptor (PTHR1) were detected using immunohistochemistry. Bcl2, which is activated by the PTHR1, was not expressed in the *EXT*^{wt/wt} and *EXT*^{wt/-} pellets nor in the OCs (Table 3).

BMP and TGF- β Signaling

Phosphosmad 1,5,8 and phosphosmad 2 staining was positive in the nucleus of cells in the *EXT*^{wt/wt} and *EXT*^{wt/-} pellets and OCs (Table 3). The *EXT*^{wt/wt} and *EXT*^{wt/-} pellets exhibited a significant ($P < 0.05$) higher mean sum score of phosphosmad 1,5,8 expression in the nucleus compared to the OCs (Figure 4, H and K). Also, plasminogen activator inhibitor 1 (PAI1) was significantly higher expressed in the cytoplasm of the *EXT*^{wt/wt} and *EXT*^{wt/-} pellets compared to the OCs (Figure 4, I and L; Table 3). Focal nuclear PAI1 expression was found in the

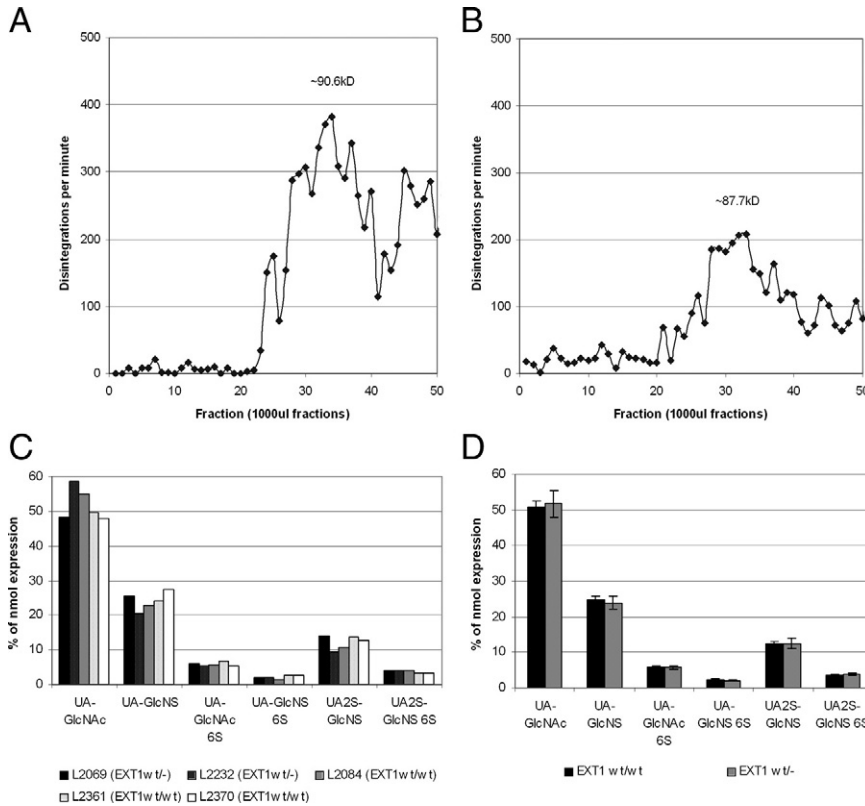


Figure 3. HS chain length and HS composition in *EXT1^{wt/wt}* and *EXT1^{wt/-}* MSCs. HS chain length was determined in *EXT1^{wt/wt}* (L2370, 89,000 dpm analyzed, size ~90.6 kDa) (A) and *EXT1^{wt/-}* (L2232, 51,600 dpm analyzed, size ~87.7 kDa) (B) MSCs on a CL-6B Sepharose column. The average HS chain size of the MSCs was estimated from extrapolation of a CL-6B Sepharose standard curve to be 80–120 kDa.⁵³ C: Relative expression of HS disaccharides per sample. D: Relative expression of HS disaccharides in *EXT1^{wt/wt}* (*n* = 3) and *EXT1^{wt/-}* MSCs (*n* = 2) as analyzed by SAX-HPLC. No significant differences were observed between *EXT1^{wt/wt}* and *EXT1^{wt/-}* MSCs. Error bars indicate the SEM.

EXT1^{wt/wt} and *EXT1^{wt/-}* pellets and the OCs. Thus, BMP- and TGF- β signaling seem to be more active in the pellets as compared to the tumor samples.

Wnt Signaling

Cytoplasmic and some nuclear β -catenin staining was observed in the *EXT1^{wt/wt}* and *EXT1^{wt/-}* pellets and OCs

(Table 3). The 2-week *EXT1^{wt/-}* pellets expressed a significant (*P* < 0.05) higher level of cytoplasmic β -catenin mean sum score than the 6-week *EXT1^{wt/-}* pellets (data not shown).

Discussion

In the present study we addressed the long-debated question of whether OCs in MO patients develop via

Table 3. Results of Immunohistochemistry of EXT-Related Genes and HS-Dependent Pathways

	<i>P</i> < 0.05	Localization						N
		Pellets (<i>EXT1^{wt/wt}</i> ; <i>EXT1^{wt/-}</i>)			OC (<i>EXT1^{-/-}</i>)			
		Cytoplasm	Nucleus	ECM	Cytoplasm	Nucleus	ECM	
NDST1	No	++	-	±	++	++	+*	9/9
SDC2	No	++	± (6 weeks)	±	++	±	-	9/9
SDC3	No	+	±	-	+	±	+*†	9/9
SDC4	No	++	-	± (2 weeks)	++	-	-	8/8
Perlecan	No	+	-	-	+	-	±*†	6/6
CD44v3	Yes	±	± [§]	± [†]	+	± [§]	±*	8/8
Phosphosmad 1,5,8	Yes	-	++	-	-	+	-	7/8
Phosphosmad 2	No	-	+	-	-	+	-	7/7
PAI1	Yes	++	±	-	+	±	-	9/9
β -Catenin	No	+	±	-	+	+	-	8/8
PTH1H	No	+	-	-	++	-	-	9/9
PTHR1	No	+	-	-	+	-	-	8/8
Bcl2	No	-	-	-	-	-	-	0/9

OC indicates osteochondroma; ECM, extracellular matrix; wk, weeks of culturing; N, number of positive OCs. ++ = strongly positive (mean sum score >5); + = positive (mean sum score 3–5); ± = focal (2); - = negative. *Pericellular. †Membranous. ‡Ossification zone; §dot-like.

Statistical analysis: one-way ANOVA, Bonferroni's Multiple comparison test in which all groups were compared; Significant differences (*P* < 0.05) were present between the pellets and OCs.

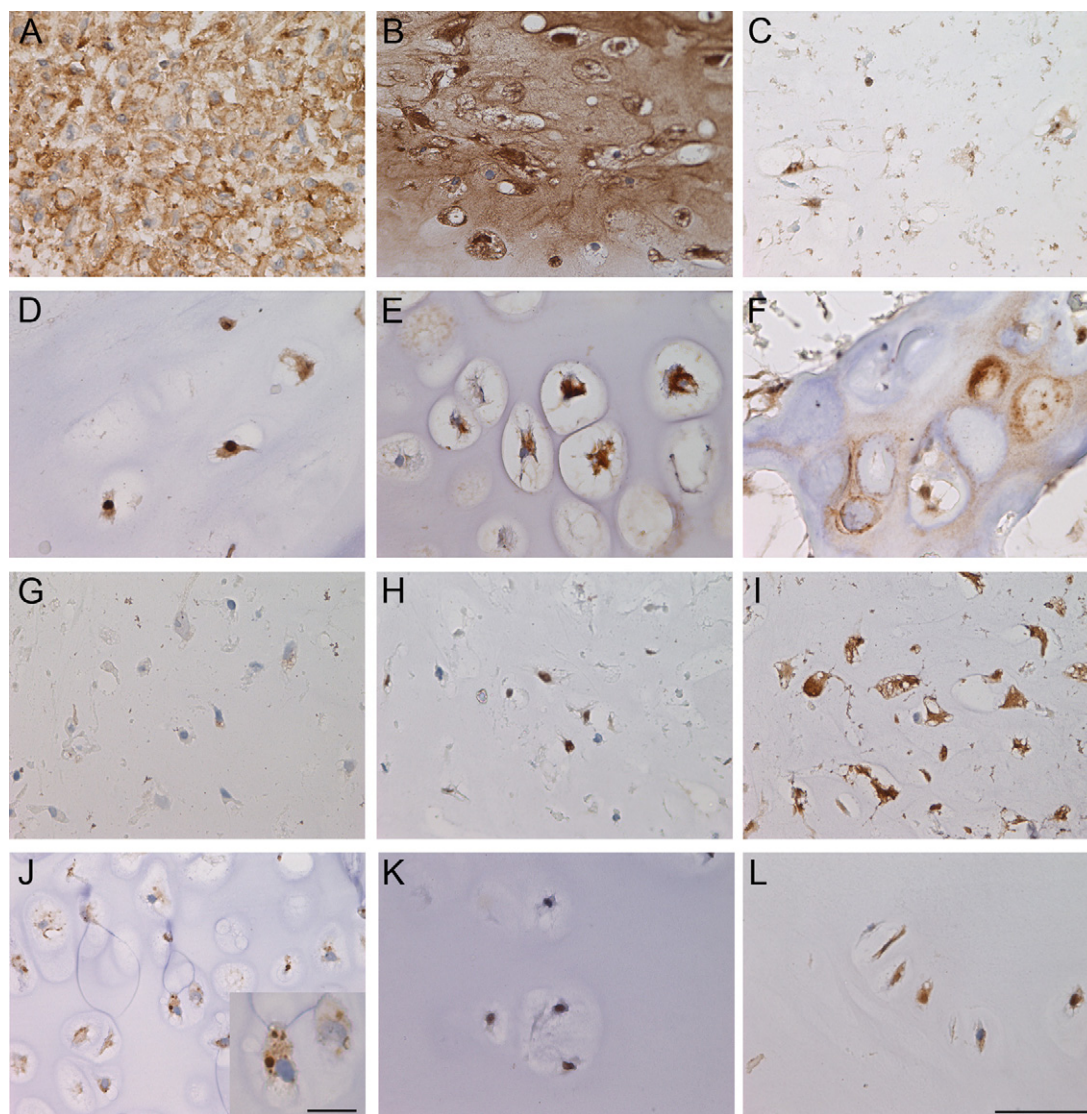


Figure 4. Protein expression of *EXT*-related genes and HS-dependent pathways in pellets and OCs. Cytoplasmic NDST1 protein expression in pellets (**A**) versus nuclear and cytoplasmic staining in the OCs (L2804; **D**). SDC2 protein expression is present in the ECM of the pellets (**B**), while absent in the OCs (L2370; **E**). SDC3 protein expression is absent in the ECM of the pellets (**C**) and present in the OCs (L2467; **F**). Cytoplasmic CD44v3 protein is predominantly expressed in OCs (dot-like; L2370; **J**) and weakly in pellets (**G**). Both BMP (nuclear phosphosmad1) and TGF- β (cytoplasmic PAI1) signaling is active in the pellets (**H** and **I**) and OCs (L2370) (**K** and **L**), respectively. Scale bars: 50 μ m (**A-L**); 10 μ m (inset **J**).

haploinsufficiency (gene dosage model, ie, the loss of one *EXT* allele)^{13,14,36} or via the classical two-hit model for tumor suppressor genes.^{5,7} Loss of heterozygosity of *EXT1* and/or *EXT2* was shown in solitary OCs⁶⁻⁸ as well as in a proportion of hereditary OCs,⁷ supporting the two-hit model. However, in a considerable number of hereditary OCs loss of the remaining wild-type allele could not be found, giving rise to the question whether OCs in MO patients could arise through haploinsufficiency. We therefore compared *EXT*, HS, HSPG, and the HS-dependent signaling pathways between cells containing a heterozygous mutation in *EXT1* or *EXT2* (*EXT*^{wt/-} MSCs of MO patients) and wild-type cells (*EXT*^{wt/wt} MSCs of healthy donors and SO patients). Results were compared to tumor tissue, in which *EXT*, at least in solitary OCs,⁸ is presumed to be homozygously affected (*EXT*^{-/-}).

In the present series the predominance of the mutated allele at DNA sequence analysis of the tumor tissue suggested loss of the remaining wild-type allele in three of five patients carrying a germline *EXT* mutation. Two of three solitary OCs demonstrated homozygous deletion of *EXT1*. *EXT* mRNA expression in these cases was diminished compared to growth plate mRNA expression and comparable to the earlier reported expression levels in OCs.²³ The fact that a second hit could be demonstrated in 63% of cases (5/8; both solitary and hereditary) is similar to published data.⁶⁻⁸

We successfully induced chondrogenesis both in *EXT*^{wt/wt} and *EXT*^{wt/-} MSCs, and cartilaginous differentiation was confirmed by metachromasia with toluidine blue and by the expression of collagen II, SOX9 and collagen X (hypertrophic differentiation). We did not observe a difference in chondrogenesis between *EXT*^{wt/wt} and *EXT*^{wt/-}

MSCs. Thus, our data indicate that inactivation of one *EXT* allele does not impair cartilage formation.

EXT1 and *EXT2* are responsible for HS chain length elongation. Here we show that the HS chain length and HS structure are identical in *EXT^{wt/wt}* and *EXT^{wt/-}* MSCs and that the HS chain length of the MSCs is within the normal range.³⁷ *EXT* mutations are reported to affect HS chain length.³⁸ *EXT1* or *EXT2* down-regulation will lead to shortened HS chains, whereas *EXT1* (and *EXT2*) overexpression will lead to elongated HS chains.³⁹ We did not observe a difference in *EXT* expression nor in HS staining between *EXT^{wt/wt}* and *EXT^{wt/-}* pellets. Our results in human differ from those in mice, of which heterozygous *Ext1*-deficient embryonic stem cells show a reduction in transferase activity and in HS level compared to wild-type cells.⁴⁰ The fact that in human HS chain length as well as its structure is normal in MSCs carrying a heterozygous *EXT* mutation supports the notion that loss of a single *EXT* allele does not affect HS biosynthesis and therefore strongly argues against haploinsufficiency. However, our results were found in MSCs in monolayer culture, and because HSPG composition is tissue-specific⁴¹ one cannot completely rule out that chain lengths are different when cells are differentiated toward cartilage. Moreover, because culturing of *EXT^{-/-}* cartilaginous cap cells failed we could not confirm and compare to a presumed reduced chain length in *EXT^{-/-}* cells.

The expression of HS, different HSPGs, as well as downstream signaling molecules was not significantly different between normal MSCs and MSCs carrying a heterozygous *EXT* mutation. Interestingly, the majority of OCs exhibited focal cytoplasmic and/or nuclear HS expression. This suggests that the cartilage cap still contains a number of nonmutated cartilaginous cells with a normal HS chain length. The localization of the HSPG protein cores differed between the pellets and OCs. The CD44v3 expression is significantly lower in the pellets as compared to the OCs. This is in line with previous data of CD44v3 expression to be significantly lower in growth plate compared to the OCs.²³ CD44v3 expression therefore seems to be tumor-specific. Of the HS dependent signaling pathways, activity of both BMP (phosphosmad 1,5,8) and TGF- β signaling (PAI1) was shown to be significantly higher in the pellets compared to the OCs. It is likely that the activity of those pathways in the pellets is (partly) caused by the supplements, TGF- β and BMP-6, which were added in the medium during *in vitro* chondrogenesis.

Thus, our data strongly argue against haploinsufficiency of *EXT1* or *EXT2* as an explanation for OC formation because HS chain length and structure, *in vitro* chondrogenesis and the expression of *EXT*, HS and *EXT* downstream molecules were identical in *EXT^{wt/-}* and *EXT^{wt/wt}* cells. However, the second hit could not be detected in 3/8 OCs in our series despite a low *EXT* expression level in those OCs. Alternative mechanisms may exist causing (near) complete inactivation of *EXT*. Epigenetic gene silencing by methylation in the *EXT1* and *EXT2* promoter region was however shown to be absent.^{23,42,43} Other alterations in or nearby the promoter region or the involvement of microRNAs cannot be excluded.

Our results, however, provide an alternative explanation for the fact that the second hit is not always detectable in OC. We observed some remaining HS expression in the cartilage cap. Furthermore, we repeatedly cultured *EXT^{wt/-}* or *EXT^{wt/wt}* cells instead of *EXT^{-/-}* cells from the carefully dissected cartilaginous cap. Moreover, *EXT* expression at mRNA level is decreased in OC, but there is always some expression remaining.²³ These data may suggest that the cartilage cap is heterogeneous in composition, comprising not only *EXT^{-/-}* tumor cells but also normal cells in between the tumor cells (mosaicism). The need for a second hit was recently confirmed in a conditional *Ext1^{+/-}* and *Ext2^{+/-}* mice do not show OCs of the long bones,^{36,40,44} complete inactivation of *EXT1* in chondrocytes results in a phenotype strongly resembling human MO.⁴⁵ Interestingly, the cartilage caps of the mouse OCs also demonstrate a mixture of mutated and normal cells indicating mosaicism.⁴⁵ This is in accordance with the zebrafish model of Clement and colleagues,⁴⁶ who suggested a loss of heterozygosity model for OC formation in which loss of polarity leads to the cartilage cap of an OC which major component consists of *EXT^{-/-}* chondrocytes and its minor component of hypertrophic *EXT^{wt/-}* chondrocytes. The HS staining of the human OCs suggests however that the normal cells are not restricted to the hypertrophic zone (as in the zebrafish model)⁴⁶ or to small single clones (as in the mouse model)⁴⁵ but are intermingled with the HS negative cells. The detection of loss of the remaining wild-type allele in OC using DNA based techniques will depend on the ratio of normal versus mutant cells.

In conclusion, we could demonstrate a second hit in the *EXT* genes in five of eight OCs, including both solitary and hereditary OCs. MSCs carrying a heterozygous *EXT* mutation are identical to wild-type MSCs with regard to HS chain length and structure, *in vitro* chondrogenesis, and the expression of *EXT*, HS, and their downstream molecules. Therefore, our results refute the haploinsufficiency theory and strongly support the two-hit model for OC formation. The heterogeneous composition of the cartilaginous cap, containing both HS-positive and HS-negative cells, suggests that the detection of the second hit in OC depends on the ratio of normal versus mutated cells in the cartilaginous cap.

Acknowledgments

We thank Armin W. Walter (Onze Lieve Vrouwe Gasthuis, Amsterdam, The Netherlands), and Antonie H. M. Taminiau for kindly providing the patient material; Sahila Balkassmi for the *EXT* mutation analysis; Daniëlle de Jong for expert assistance with the DNA tiling array; Helene Roelofs for providing the healthy donor MSCs; Jarom Heijmans for the IHH primers; Razvan L. Miclea, Salvatore Romeo, and Malgorzata Wiweger for their expertise; Brendy van den Akker, Maayke van Ruler, Hans J. Baelde, Inge Briaire-de Bruijn, Ronald Duim, and Marcel Winter for their practical assistance; and Frans Prins for his professional help with the spectral imaging.

References

1. Khurana J, Abdul-Karim F, Bovée JVMG: Osteochondroma. World Health Organization classification of tumours. Pathology and genetics of tumours of soft tissue and bone. Edited by CDM Fletcher, KK Unni, and F Mertens. Lyon, France, IARC Press, 2002, pp. 234–236
2. Bovée JVMG Hogendoorn PCW: Congenital and inherited syndromes associated with bone and soft tissue tumours: Multiple osteochondromas. World Health Organisation classification of tumours. Pathology and genetics of tumours of soft tissue and bone. Edited by CDM Fletcher, KK Unni, and F Mertens. Lyon, France, IARC Press, 2002, pp. 360–362
3. Legeai-Mallet L, Munnich A, Maroteaux P, Le Merrer M: Incomplete penetrance and expressivity skewing in hereditary multiple exostoses. *Clin Genet* 1997, 52:12–16
4. Bovée JVMG: Multiple osteochondromas. *Orphanet J Rare Dis* 2008, 3:3
5. Knudson AG Jr: Mutation and cancer: statistical study of retinoblastoma. *Proc Natl Acad Sci USA* 1971, 68:820–823
6. Bernard MA, Hall CE, Hogue DA, Cole WG, Scott A, Snuggs MB, Clines GA, Ludecke HJ, Lovett M, Van Winkle WB, Hecht JT: Diminished levels of the putative tumor suppressor proteins EXT1 and EXT2 in exostosis chondrocytes. *Cell Motil Cytoskeleton* 2001, 48:149–162
7. Bovée JVMG, Cleton-Jansen AM, Wuyts W, Caethoven G, Taminiau AHM, Bakker E, Van Hul W, Cornelisse CJ, Hogendoorn PCW: EXT-mutation analysis and loss of heterozygosity in sporadic and hereditary osteochondromas and secondary chondrosarcomas. *Am J Hum Genet* 1999, 65:689–698
8. Hameetman L, Szuhai K, Yavas A, Knijnenburg J, van Duin M, Van Dekken H, Taminiau AHM, Cleton-Jansen AM, Bovée JVMG, Hogendoorn PCW: The role of EXT1 in nonhereditary osteochondroma: identification of homozygous deletions. *J Natl Cancer Inst* 2007, 99:396–406
9. Hallor KH, Staaf J, Bovée JVMG, Hogendoorn PCW, Cleton-Jansen AM, Knuutila S, Savola S, Niini T, Brosjo O, Bauer HCF, Vult von Steyern F, Jonsson K, Skorpil M, Mandahl N, Mertens F: Genomic profiling of chondrosarcoma: chromosomal patterns in central and peripheral tumors. *Clin Cancer Res* 2009, 15:2685–2694
10. Hecht JT, Hogue D, Strong LC, Hansen MF, Blanton SH, Wagner M: Hereditary multiple exostosis and chondrosarcoma: linkage to chromosome 11 and loss of heterozygosity for EXT-linked markers on chromosomes 11 and 8. *Am J Hum Genet* 1995, 56:1125–1131
11. Raskind WH, Conrad EU, Chansky H, Matsushita M: Loss of heterozygosity in chondrosarcomas for markers linked to hereditary multiple exostoses loci on chromosomes 8 and 11. *Am J Hum Genet* 1995, 56:1132–1139
12. Bernard MA, Hogue DA, Cole WG, Sanford T, Snuggs MB, Montufar-Solis D, Duke PJ, Carson DD, Scott A, Van Winkle WB, Hecht JT: Cytoskeletal abnormalities in chondrocytes with EXT1 and EXT2 mutations. *J Bone Miner Res* 2000, 15:442–450
13. Hall CR, Cole WG, Haynes R, Hecht JT: Reevaluation of a genetic model for the development of exostosis in hereditary multiple exostosis. *Am J Med Genet* 2002, 112:1–5
14. Legeai-Mallet L, Rossi A, Benoist-Lasselin C, Piazza R, Mallet JF, Delezoid AL, Munnich A, Bonaventure J, Zylberberg L: EXT 1 gene mutation induces chondrocyte cytoskeletal abnormalities and defective collagen expression in the exostoses. *J Bone Miner Res* 2000, 15:1489–1500
15. Lind T, Tufaro F, McCormick C, Lindahl U, Lidholt K: The putative tumor suppressors EXT1 and EXT2 are glycosyltransferases required for the biosynthesis of heparan sulfate. *J Biol Chem* 1998, 273:26265–26268
16. McCormick C, Leduc Y, Martindale D, Mattison K, Esford LE, Dyer AP, Tufaro F: The putative tumour suppressor EXT1 alters the expression of cell-surface heparan sulfate. *Nat Genet* 1998, 19:158–161
17. McCormick C, Duncan G, Goutsos KT, Tufaro F: The putative tumor suppressors EXT1 and EXT2 form a stable complex that accumulates in the golgi apparatus and catalyzes the synthesis of heparan sulfate. *Proc Natl Acad Sci USA* 2000, 97:668–673
18. Simmons AD, Musy MM, Lopes CS, Hwang L-Y, Yang Y-P, Lovett M: A direct interaction between EXT proteins and glycosyltransferases is defective in hereditary multiple exostoses. *Hum Mol Genet* 1999, 8:2155–2164
19. Bellaïche Y, The I, Perrimon N: Tout-velu is a drosophila homologue of the putative tumour suppressor EXT1 and is needed for Hh diffusion. *Nature* 1998, 394:85–88
20. Han C, Belenkaya TY, Khodoun M, Tauchi M, Lin X, Lin X: Distinct and collaborative roles of Drosophila EXT family proteins in morphogen signalling and gradient formation. *Development* 2004, 131:1563–1575
21. Takei Y, Ozawa Y, Sato M, Watanabe A, Tabata T: Three Drosophila EXT genes shape morphogen gradients through synthesis of heparan sulfate proteoglycans. *Development* 2004, 131:73–82
22. Toyoda H, Kinoshita-Toyoda A, Selleck SB: Structural analysis of glycosaminoglycans in drosophila and caenorhabditis elegans and demonstration that tout-velu, a drosophila gene related to EXT tumor suppressors, affects heparan sulfate in vivo. *J Biol Chem* 2000, 275:2269–2275
23. Hameetman L, David G, Yavas A, White SJ, Taminiau AHM, Cleton-Jansen AM, Hogendoorn PCW, Bovée JVMG: Decreased EXT expression and intracellular accumulation of heparan sulphate proteoglycan in osteochondromas and peripheral chondrosarcomas. *J Pathol* 2007, 211:399–409
24. Benoist-Lasselin C, de Margerie E, Gibbs L, Cormier S, Silve C, Nicolas G, Lemerrer M, Mallet JF, Munnich A, Bonaventure J, Zylberberg L, Legeai-Mallet L: Defective chondrocyte proliferation and differentiation in osteochondromas of MHE patients. *Bone* 2006, 39:17–26
25. Hameetman L, Rozeman LB, Lombaerts M, Oosting J, Taminiau AHM, Cleton-Jansen AM, Bovée JVMG, Hogendoorn PCW: Peripheral chondrosarcoma progression is accompanied by decreased Indian Hedgehog (IHH) signalling. *J Pathol* 2006, 209:501–511
26. Bovée JVMG, Van den Broek LJC, Cleton-Jansen AM, Hogendoorn PCW: Up-regulation of PTHrP and Bcl-2 expression characterizes the progression of osteochondroma towards peripheral chondrosarcoma and is a late event in central chondrosarcoma. *Lab Invest* 2000, 80:1925–1933
27. Hameetman L, Kok P, Eilers PHC, Cleton-Jansen AM, Hogendoorn PCW, Bovée JVMG: The use of Bcl-2 and PTHLH immunohistochemistry in the diagnosis of peripheral chondrosarcoma in a clinicopathological setting. *Virchows Arch* 2005, 446:430–437
28. Vink GR, White SJ, Gabelic S, Hogendoorn PCW, Breuning MH, Bakker E: Mutation screening of EXT1 and EXT2 by direct sequence analysis and MLPA in patients with multiple osteochondromas: splice site mutations and exonic deletions account for more than half of the mutations. *Eur J Hum Genet* 2004, 13:470–474
29. White SJ, Vink GR, Kriek M, Wuyts W, Schouten J, Bakker B, Breuning MH, den Dunnen JT: Two-color multiplex ligation-dependent probe amplification: detecting genomic rearrangements in hereditary multiple exostoses. *Hum Mutat* 2004, 24:86–92
30. Schrage YM, Hameetman L, Szuhai K, Cleton-Jansen AM, Taminiau AHM, Hogendoorn PCW, Bovée JVMG: Aberrant heparan sulfate proteoglycan localization, despite normal exostosin, in central chondrosarcoma. *Am J Pathol* 2009, 174:979–988
31. Chen E, Stringer SE, Rusch MA, Selleck SB, Ekker SC: A unique role for 6-O sulfation modification in zebrafish vascular development. *Dev Biol* 2005, 284:364–376
32. Robinson CJ, Mulloy B, Gallagher JT, Stringer SE: VEGF165-binding sites within heparan sulfate encompass two highly sulfated domains and can be liberated by K5 lyase. *J Biol Chem* 2006, 281:1731–1740
33. Wasteson A: A method for the determination of the molecular weight and molecular-weight distribution of chondroitin sulphate. *J Chromatogr* 1971, 59:87–97
34. David G, Bai XM, Van der Schueren B, Marynen P, Cassiman JJ, Van den Berghe H: Spatial and temporal changes in the expression of fibroglycan (syndecan-2) during mouse embryonic development. *Development* 1993, 119:841–854
35. Bovée JVMG, Cleton-Jansen AM, Kuipers-Dijkshoorn N, Van den Broek LJC, Taminiau AHM, Cornelisse CJ, Hogendoorn PCW: Loss of heterozygosity and DNA ploidy point to a diverging genetic mechanism in the origin of peripheral and central chondrosarcoma. *Genes Chrom Cancer* 1999, 26:237–246
36. Stickens D, Zak BM, Rougier N, Esko JD, Werb Z: Mice deficient in Ext2 lack heparan sulfate and develop exostoses. *Development* 2005, 132:5055–5068
37. Knox S, Merry C, Stringer SE, Melrose J, Whitelock J: Not all perlecanans are created equal: interactions with fibroblast growth factor (FGF) 2 and FGF receptors. *J Biol Chem* 2002, 277:14657–14665
38. Yamada S, Busse M, Ueno M, Kelly OG, Skarnes WC, Sugahara K,

- Kusche-Gullberg M: Embryonic fibroblasts with a gene trap mutation in EXT1 produce short heparan sulphate chains. *J Biol Chem* 2004, 279:32134–32141
39. Busse M, Feta A, Presto J, Wilen M, Gronning M, Kjellen L, Kusche-Gullberg M: Contribution of EXT1, EXT2, and EXTL3 to heparan sulfate chain elongation *J Biol Chem* 2007, 282:32802–32810
 40. Lin X, Wei G, Shi Z, Dryer L, Esko JD, Wells DE, Matzuk MM: Disruption of gastrulation and heparan sulfate biosynthesis in EXT1-deficient mice. *Dev Biol* 2000, 224:299–311
 41. Shi X, Zaia J: Organ-specific heparan sulfate structural phenotypes. *J Biol Chem* 2009, 284:11806–11814
 42. Roper S, Setien F, Espada J, Fraga MF, Herranz M, Asp J, Benassi MS, Franchi A, Patino A, Ward LS, Bovée J, Igudosa JC, Im W, Steller M: Epigenetic loss of the familial tumor-suppressor gene exostosin-1 (EXT1) disrupts heparan sulfate synthesis in cancer cells. *Hum Mol Genet* 2004, 13:2753–2765
 43. Tsuchiya T, Osanai T, Ogoe A, Tamura G, Chano T, Kaneko Y, Ishikawa A, Orui H, Wada T, Ikeda T, Namba M, Takigawa M, Kawashima H, Hotta T, Tsuchiya A, Ogino T, Motoyama T: Methylation status of EXT1 and EXT2 promoters and two mutations of EXT2 in chondrosarcoma. *Cancer Genet Cytogenet* 2005, 158:148–155
 44. Hilton MJ, Gutierrez L, Martinez DA, Wells DE: EXT1 regulates chondrocyte proliferation and differentiation during endochondral bone development. *Bone* 2005, 36:379–386
 45. Jones KB, Piombo V, Searby C, Kurriger G, Yang B, Grabellus F, Roughley PJ, Morcuende JA, Buckwalter JA, Capecchi MR, Vortkamp A, Sheffield VC: A mouse model of osteochondromagenesis from clonal inactivation of Ext1 in chondrocytes. *Proc Natl Acad Sci USA* 2010, 107:2054–2059
 46. Clement A, Wiweger M, von der HS, Rusch MA, Selleck SB, Chien CB, Roehl HH: Regulation of zebrafish skeletogenesis by ext2/dackel and papst1/pinscher. *PLoS Genet* 2008, 4:e1000136